1976, *Astron. Astrophys. Suppl.* **23**, 13-35.

MONOCHROMATIC AND WHITE-LIGHT OBSERVATIONS OF COMET BENNETT 1969i (1970II)

J. RAHE*, C.W. McCRACKEN** and B.D. DONN***
NASA-Goddard Space Flight Center, Greenbelt, USA

Received June 5, 1974

Isophotes have been determined from 32 photographs of Comet Bennett 1969i (1970II) taken during the period March 28 to April 18, 1970. The six interference filters used were centered on the CN λ3883Å, C_2 λ4737Å, C_2 λ5165Å, CO^+ λ4277Å sequences, on the sodium-D-lines at λ5893Å, and on the continuum at λ5300Å. Intensity gradients have been derived from these isophotes.

Key words: Comet Bennett 1969i (1970II) – monochromatic observations-comets-isophotes of comets

1. OBSERVATIONS

The orbital parameters of Comet Bennett 1969i (1970II) given by Marsden (1972) are:

$$e = 0.996$$
$$q = 0.538 \text{ AU}$$
$$\omega = 354\overset{\circ}{.}2$$
$$\Omega = 224\overset{\circ}{.}0$$
$$i = 90\overset{\circ}{.}05$$
$$T = 1970, \text{ March } 20.046 \text{ ET.}$$

Twenty-seven photographs suitable for reduction were obtained between March 27-28, 1970 and April 17-18, 1970 with the 91 cm (36″) f/14.3 reflector at the Goddard Space Flight Center. During this time interval, the heliocentric distance, r, and geocentric distance, Δ, of the comet varied between $0.572 \leq r \leq 0.846$ AU and $0.693 \leq \Delta \leq 1.063$ AU. The exposure times of the photographs varied between 30 sec. and 10 min. The background densities of the original plates varied considerably because of changing sky brightness during the twilight observing sessions.

The photographs taken during March were direct images on Kodak IIIa-J, IIa-O, and Ia-E emulsions. Those obtained in April were taken with an image intensifier which had an S-20 photocathode. A detailed description of the equipment used and of the method of reduction is given in the preceding paper (Rahe *et al.* 1976, Paper I). Several interference filters were selected to study the continuum at λ5300Å, the C_2 (0,0) and C_2 (1,0) Swan band sequences at λ4737Å and λ5165Å, the CN (0,0) violet band at λ3883Å, the CO+ (2,0) Comet Tail band at λ4267Å, and the sodium-D-lines at λ5893Å. Table 1 gives the filter designation, wavelength of maximum transmission, full width at half maximum, peak transmission in percent, and the cometary emission observed for each of the filters. The CO^+ filter was manufactured by Spectrum Systems, Inc.; the others were made by Thin-Film Products, Inc.

Table 2 is a log of the monochromatic photographs. The first column gives the number of the figure showing the isophotes; this is followed by the time of mid-exposure, exposure time, emulsion, filter, and the heliocentric and geocentric distances of the comet.

On April 8 and 9, 1970, 10 photographs of the head region of Comet Bennett were obtained by H. Neckel on Kodak IIa-O plates at the Cassegrain focus of the one meter f/15 telescope at Hamburg Observatory in Hamburg-Bergedorf. The plates were taken in white light without any filter. The exposure times varied between 2 sec. and 16 min. The plates were calibrated with a spot sensitometer. Table 3 gives the data for these photographs.

* On leave from Institut für Astrophysik, Technische Universität Berlin, Germany.
** Laboratory for Optical Astronomy.
*** Laboratory for Extraterrestrial Physics.

2. REDUCTION OF OBSERVATIONS

Figures 1 through 32 present the isophotes from the photographs. The isophotal contours were derived in the same way as described in paper I. The comet-sun direction has been marked in figures 1 through 27. Because of some uncertainty in the orientation of the plates within the plate holder, the directions are accurate only to within a few degrees for these figures. North is up and east to the left in figures 28 through 32. The scales on the ordinates and abscissae give the distance from the nucleus in units of 10^3 km. The nucleus is defined as the point of greatest brightness. The number assigned to each isophotal contour gives the corresponding intensity in arbitrary units. The isophotes in the diagrams are restricted to the unvignetted region on the image tube plates.

On the plates corresponding to figures 1, 6, and 12, the background densities were above the density of the calibration step wedge. The calibrations for these cases were made with a neutral density filter (Wratten 96) placed over the calibration wedge. This procedure allows one to determine density contours but leaves the intensity contours in question. For these photographs, therefore, only density contours have been plotted. The density changes by the same amount between consecutive contours.

Figures 33 through 37 illustrate for the various emissions observed (figures 1 through 27) the decrease in intensity with increasing distance from the nucleus measured along the sun-comet line (toward the sun, left side; away from the sun, right side). The scale on the abscissa gives the distance from the nucleus in units of 10^3 km; the ordinate the logarithm of the relative intensity in arbitrary units.

3. SPECTRUM AND DUST CONTAMINATION

The spectrum of Comet Bennett showed a strong continuum (Stokes 1972) and the Comet had a prominent dust tail. Because of the extended dust coma and its strong continuum, photographs nominally taken using molecular emissions are subject to appreciable contamination. The interpretation of the Comet Bennett isophotes are therefore more difficult than those for Comet Tago-Sato-Kosaka described in paper I.

4. DISCUSSION OF THE OBSERVATIONS

A detailed analysis and discussion of the material presented here are currently being carried out and will be published later. Some preliminary descriptive remarks about the isophotes and profiles now can, however, be presented.

A comparison of figures 1 and 2 shows a remarkable similarity for nucleocentric distances up to 10^5 km. This is suggestive of a connection between sodium and dust in comets and indicates the importance of further study of this question. In particular, the continuum contribution must be kept small in order to obtain definite sodium distributions. The sodium isophotes shown here are flattened in the antisolar direction. This is particularly noticeable at small distances. The sodium isophotes are displayed in figures 2, 3, 4, 11, 17, 20, and 21. The flattened isophotes are noticeable in all the figures except figure 18 which is somewhat anomalous. The background density for this plate was very high and may have affected the isophotes. A sodium tail is quite apparent in figure 21.

At small distances from the nucleus, the Na intensity gradient is very steep in both the solar and anti-solar directions. Beyond 5 000 km the gradient in the anti-solar direction becomes much smaller showing the sodium tail. These gradients are shown in figures 33-37.

The CN isophotes in figures 9, 15 and 26 are essentially circular out to 30000 km. They become elongated in the antisolar direction beyond this distance. This behavior is unlike the nearly circular isophotes for Comet Tago-Sato-Kosaka out to about 10^5 km (Paper I). This suggests that the dust in Comet Bennett

influences the CN isophotes. One way for this to occur is contamination of the CN radiation by the dust continuum. This hypothesis appears to be inconsistent with the circular isophotes for CN within 30000 km and the very distorted continuum isophotes in the same region (figure 19) as the continuum falls off more rapidly in the anti-solar direction (figure 37). Another possible mechanism is a physical association of the source of CN with dust. Delsemme and Wenger (1970) have proposed such a connection of radicals and dust.

The isophotes for the two C_2 bands (figures 7, 8, 13, 22, 23; 5, 14, 24, and 25) are very similar to one other and to the CN isophotes.

The continuum contours for Comet Bennett resemble those of Comet Tago-Sato-Kosaka (Paper I). They are flattened near the nucleus in the antisolar direction and have a steep gradient. The gradient becomes small beyond about 50000 km, and the isophotes spread out with the beginning of the dust tail.

The shape of CO^+ isophotes close to the nucleus (within about 24000 km) falls between the circular CN and C_2 isophotes and the compressed continuum isophotes in the anti-solar direction (figures 6, 10, 16, and 27). At greater distances the contours become extended with the beginning of the ion tail. Figure 10 shows a narrow CO^+ feature starting at 25000 km with a split structure appearing at 10^5 km. This feature is visible on the original plate.

ACKNOWLEDGEMENTS

The authors thank Dr. H. Neckel, Hamburg-Bergedorf, for kindly letting them use his material. One of us (JR) was supported by NASA-Grant NGL 21-002-033, while working at the Goddard Space Flight Center. Ms. Karen Celentano, a summer student working under a National Science Foundation grant to American University, assisted in the early stages of this work. We wish to thank Dr. Kent Ford of the Department of Terrestrial Magnetism, Carnegie Institution of Washington, for the loan of the guide box. The valuable support provided by Mr. P. Taylor, the Observatory Night Assistant, during the observing sessions is gratefully acknowledged.

REFERENCES

Delsemme, A.H. and Wenger, A.: 1970, *Planet. Space Sci.* **18**, 709.
Marsden, B.G.: 1972, *Catalogue of Cometary Orbits*, Smithsonian Astrophysical Observatory, Cambridge, USA.
Rahe, J., McCracken, C.W., Hallam, K.L. and Donn, B.D.: 1976, *Astron. Astrophys. Suppl.* **23**, (Paper I).
Stockes, G.M.: *Astrophys. J.* **177**, 829.

J. Rahe
Astronomisches Institut
der Universität Erlangen-Nürnberg
und Remeis-Sternwarte Bamberg
Sternwartstr. 7
D - 8600 Bamberg, Germany

C.W. McCracken, Code 672
Laboratory for Optical Astronomy
Goddard Space Flight Center
Greenbelt, Maryland 20771, USA

B.D. Donn, Code 691
Laboratory for Extraterrestrial Physics
Goddard Space Flight Center
Greenbelt, Maryland 20771, USA

Table 1 Wavelengths of maximum transmission (λ_C). Full width at half maximum (FWHM), and peak transmission (T_C), of the interference filters, and corresponding cometary emission

Filter	λ_C(Å)	FWHM(Å)	T_C(%)	Cometary Emission
CN	3884	74	43	CN-Violet band $B^2\Sigma - X^2\Sigma$, (0,0)
C_2	4738	54	76	C_2 - Swan system $A^3\Pi - X^3\Pi$, (1,0)
C_2	5172	51	73	C_2 - Swan system $A^3\Pi - X^3\Pi$, (0,0)
CO^+	4267	20	65	CO^+ Comet Tail band $A^2\Pi - X^2\Pi$, (2,0)
Na	5893	10		Na -D lines
Con	5300	50	81	Continuum

Table 2 Monochromatic photographs of Comet Bennett 1969i (1970II)

Figure Number	Date (UT) (Middle of Exposure)	Exposure Time (Minutes)	Emulsion (Kodak)	Filter (λ_C in Å)	r (AU)	Δ (AU)
	1970					
1	March 28.417	4	IIIa-J	-	0.572	0.693
2	28.423	10	Ia-E	Na 5893	0.572	0.693
3	March 30.402	2	Ia-E	Na 5893	0.589	0.705
4	30.410	10	Ia-E	Na 5893	0.589	0.705
5	30.423	2	Ia-E	C_2 5172	0.589	0.705
6	30.430	5	Ia-O	CO^+4267	0.589	0.705
7	April 16.387	2	IIa-O	C_2 4738	0.815	1.015
8	16.392	2	IIa-O	C_2 5172	0.815	1.015
9	16.398	3	IIa-O	CN 3884	0.815	1.015
10	16.402	3	IIa-O	CO^+4267	0.815	1.015
11	16.407	2	IIa-O	Na 5893	0.815	1.015
12	16.410	2	IIa-O	Con5300	0.815	1.015
13	April 17.383	3	IIa-O	C_2 5172	0.830	1.038
14	17.387	3	IIa-O	C_2 4738	0.830	1.038
15	17.394	5	IIa-O	CN 3884	0.830	1.039
16	17.400	5	IIa-O	CO^+4267	0.830	1.039
-	17.404	1	IIa-O	CO^+4267	0.831	1.039
17	17.408	2	IIa-O	Na 5893	0.831	1.039
18	17.412	0.5	IIa-O	Con5300	0.831	1.039
19	April 18.356	0.5	IIa-O	Con5300	0.846	1.062
20	18.365	0.5	IIa-O	Na 5893	0.846	1.062
21	18.368	5	IIa-O	Na 5893	0.846	1.062
22	18.374	0.5	IIa-O	C_2 5172	0.846	1.062
23	18.377	5	IIa-O	C_2 5172	0.846	1.062
24	18.383	0.5	IIa-O	C_2 4738	0.846	1.062
25	18.385	5	IIa-O	C_2 4738	0.846	1.062
26	18.392	5	IIa-O	CN 3884	0.846	1.062
27	18.400	1	IIa-O	CO^+4267	0.846	1.063
-	18.404	10	IIa-O	CO^+4267	0.846	1.063

Table 3 White light photographs of Comet Bennett 1969i (1970II)

Figure Number	Date (UT) (Middle of Exposure)	Exposure Time	Emulsion (Kodak)
	1970		
-	April 8.092	8 min	IIa-O
28	8.121	16 min	IIa-O
-	8.136	4 min	IIa-O
29	8.142	1 min	IIa-O
-	April 9.080	6 sec	IIa-O
30	9.086	20 sec	IIa-O
-	9.093	1 min	IIa-O
31	9.099	4 min	IIa-O
32	9.110	16 min	IIa-O
-	9.120	2 sec	IIa-O

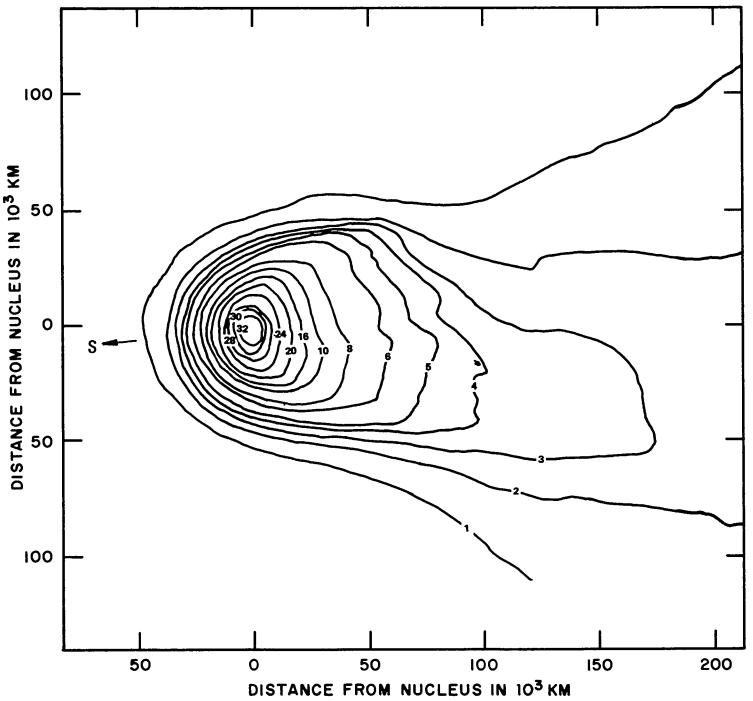

Figure 1 Density contours for photograph taken in white light without filter, March 28.417 UT, 1970, $r=0.572$ AU, $\Delta=0.693$ AU.

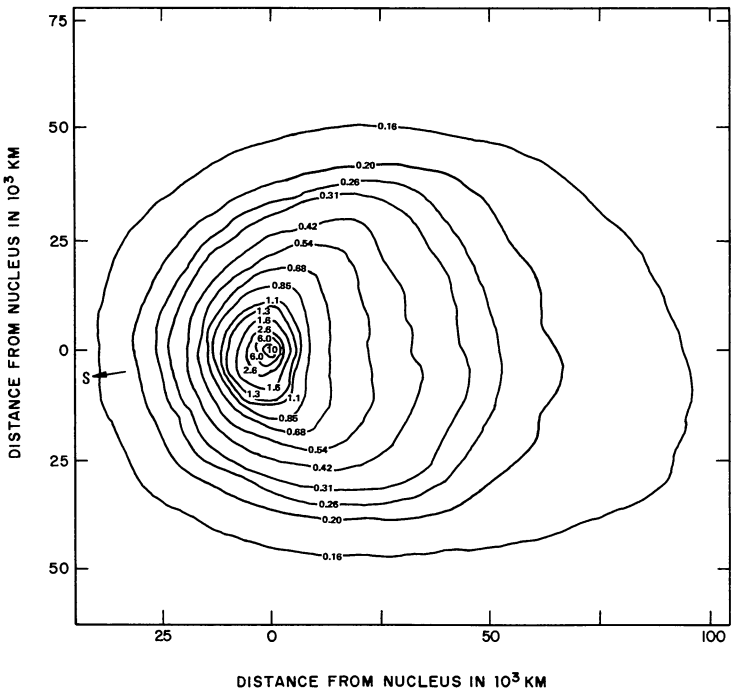

Figure 2 Isophotes for Na λ5893Å, March 28.423 UT, 1970, $r=0.572$ AU, $\Delta=0.693$ AU.

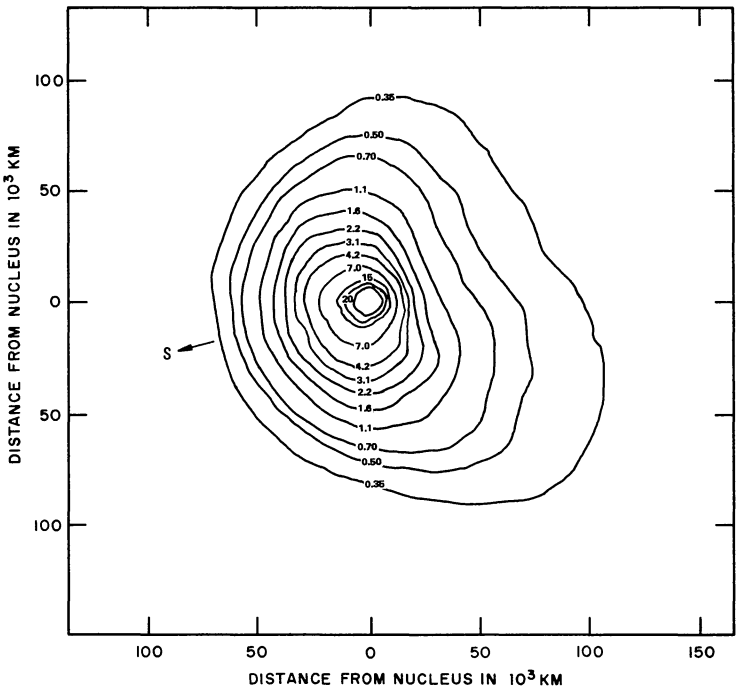

Figure 3 Isophotes for Na λ5893Å, March 30.402 UT, 1970, $r=0.589$ AU, $\Delta=0.705$ AU.

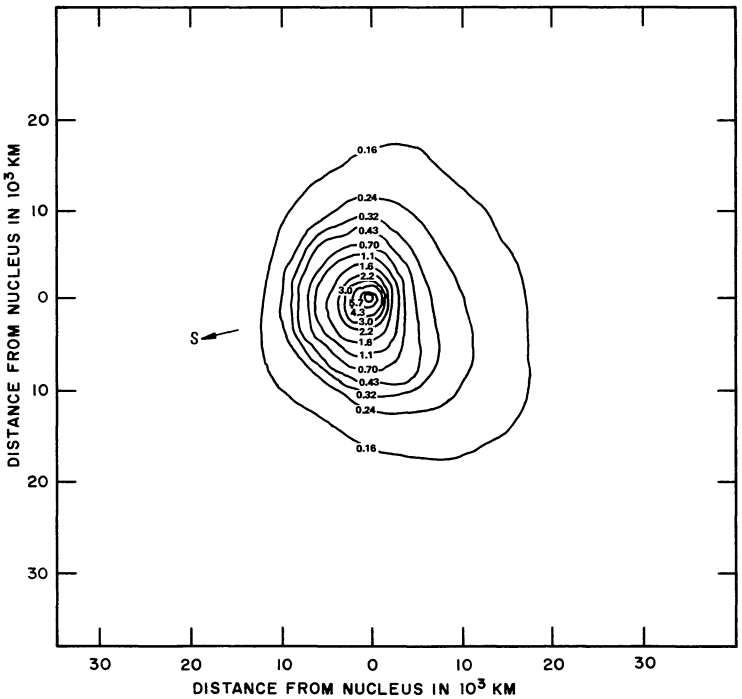

Figure 4 Isophotes for Na λ5893Å, March 30.410 UT, 1970, $r=0.589$ AU, $\Delta=0.705$ AU.

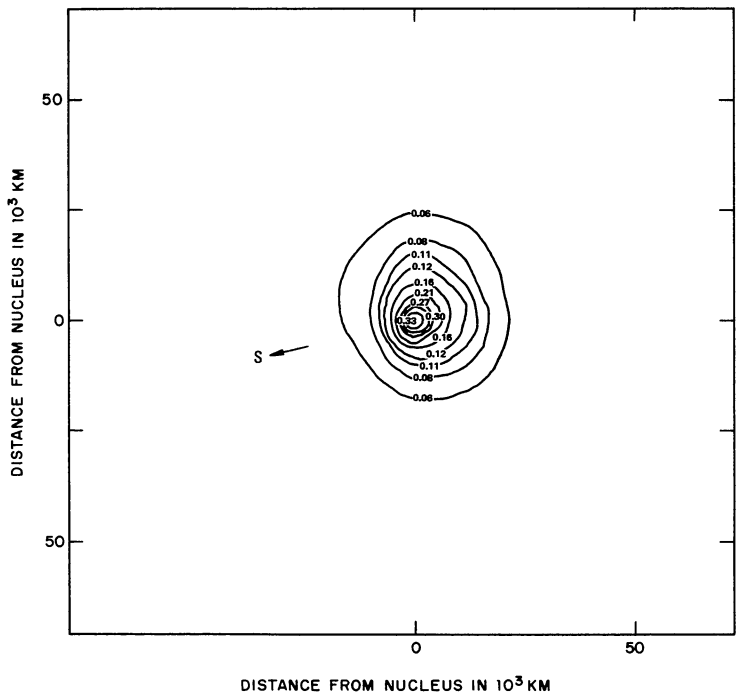

Figure 5 Isophotes for C_2 λ5172Å, March 30.423 UT, 1970, $r=0.589$ AU, $\Delta=0.705$ AU.

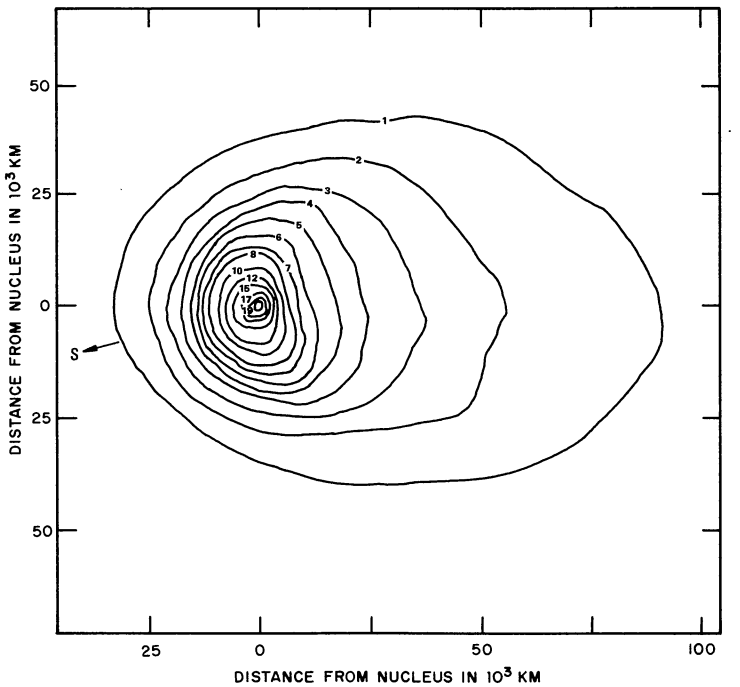

Figure 6 Density contours for CO^+ λ4267Å, March 30.430 UT, 1970, $r=0.589$ AU, $\Delta=0.705$ AU.

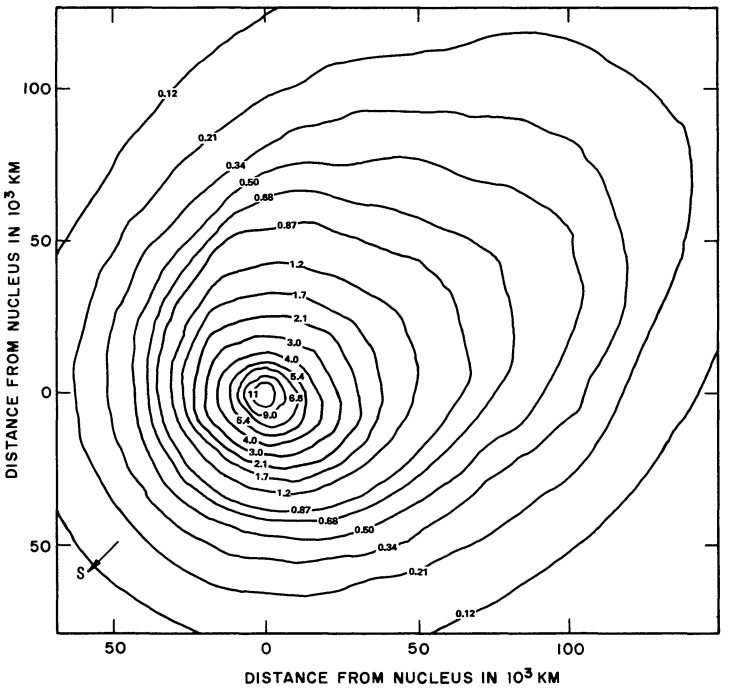

Figure 7 Isophotes for C_2 λ4738Å, April 16.387 UT, 1970, $r=0.815$ AU, $\Delta=1.015$ AU.

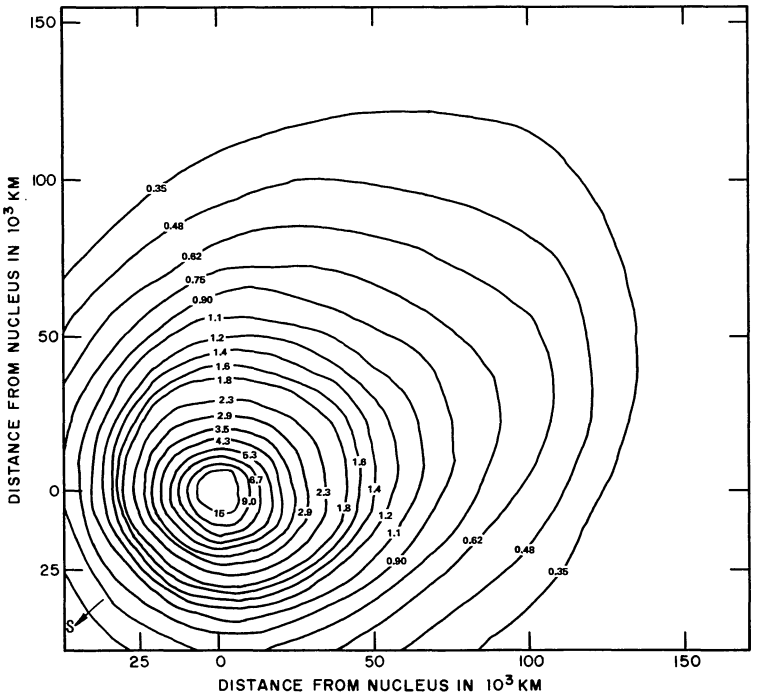

Figure 8 Isophotes for C_2 λ5172Å, April 16.392 UT, 1970, $r=0.815$ AU, $\Delta=1.015$ AU.

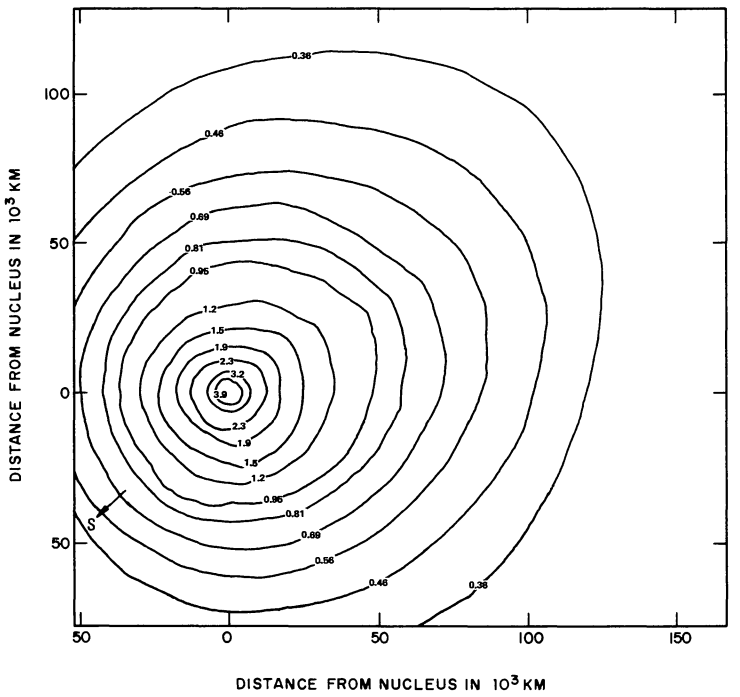

Figure 9 Isophotes for CN λ3884Å, April 16.398 UT, 1970, $r=0.815$ AU, $\Delta=1.015$ AU.

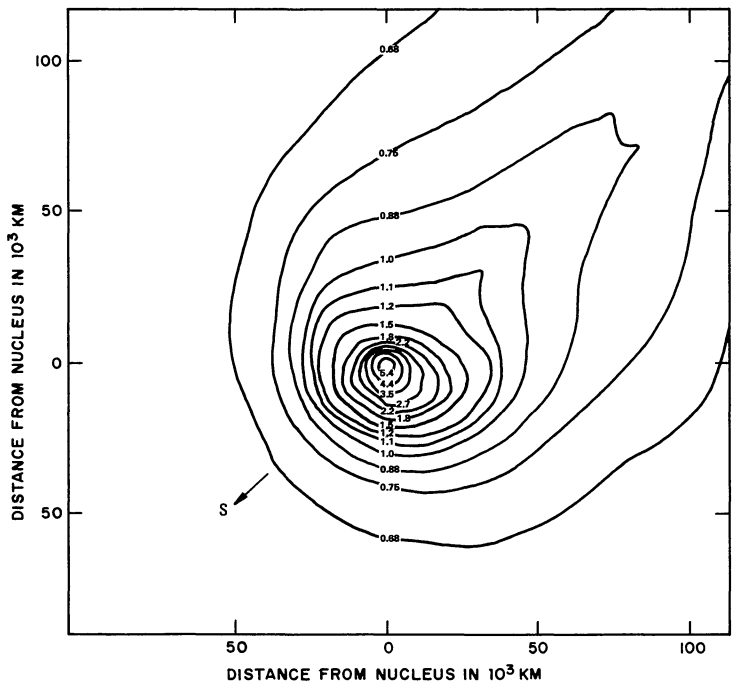

Figure 10 Isophotes for CO^+ λ4267Å, April 16.402 UT, 1970, $r=0.815$ AU, $\Delta=1.015$ AU.

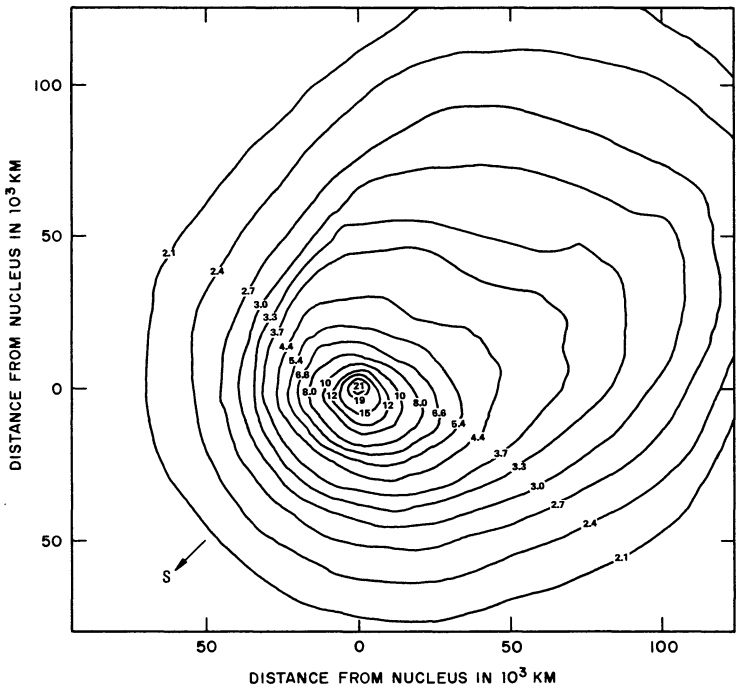

Figure 11 Isophotes for Na λ5893Å, April 16.407 UT, 1970, $r=0.815$ AU, $\Delta=1.015$ AU.

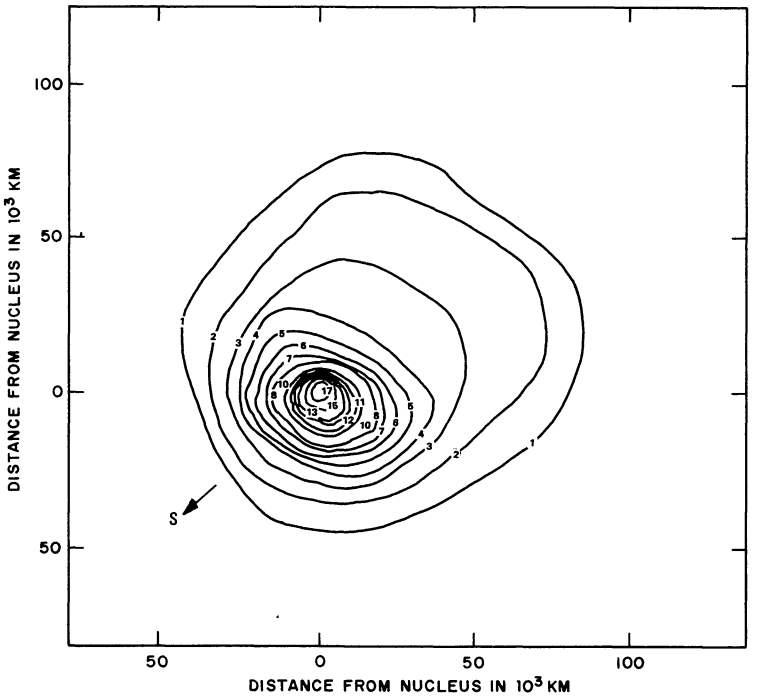

Figure 12 Density contours for continuum λ5300Å, April 16.410 UT, 1970, $r=0.815$ AU, $\Delta=1.015$ AU.

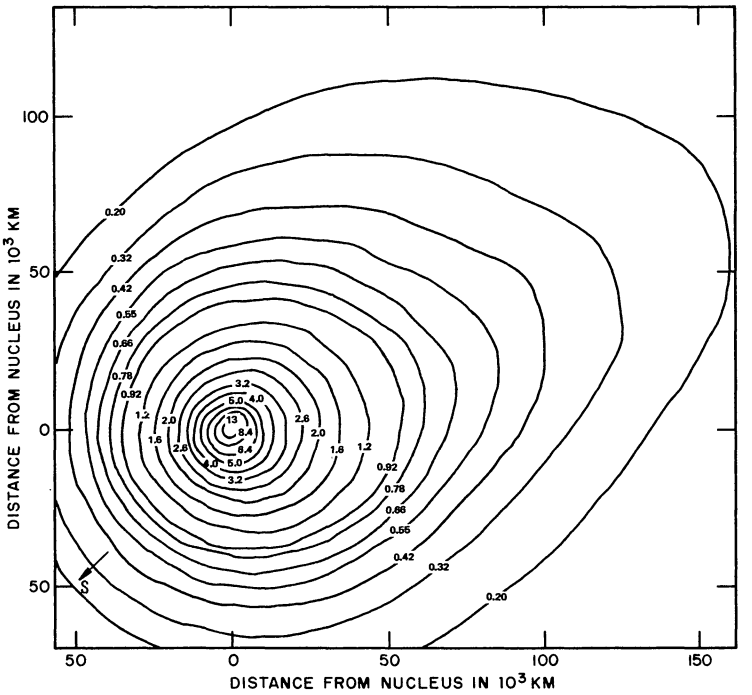

Figure 13 Isophotes for C_2 λ5172Å, April 17.383 UT, 1970, $r = 0.830$ AU, $\Delta = 1.038$ AU.

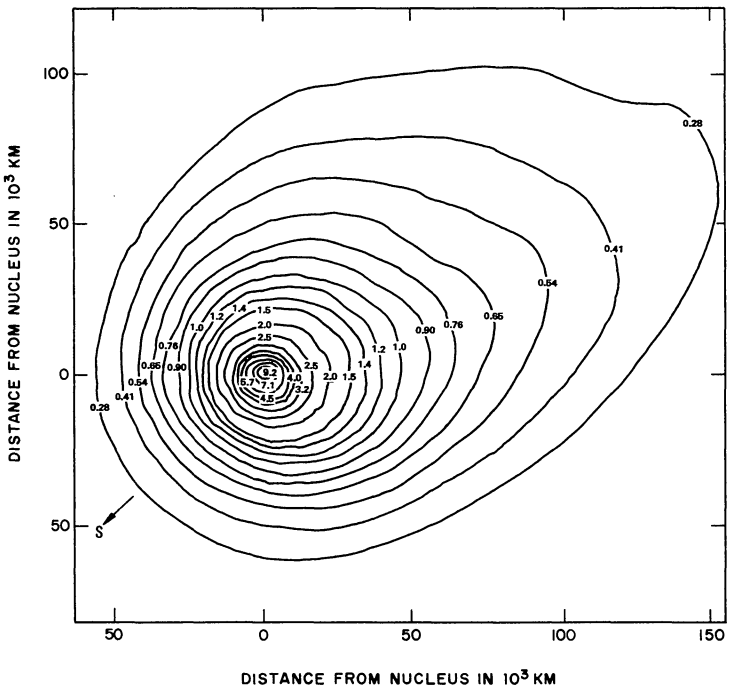

Figure 14 Isophotes for C_2 λ4738Å, April 17.387 UT, 1970, $r = 0.830$ AU, $\Delta = 1.038$ AU.

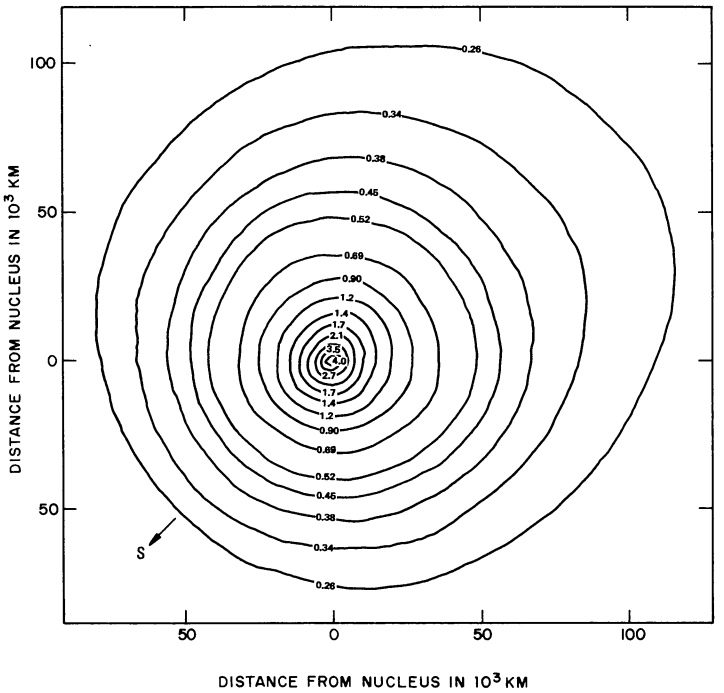

Figure 15 Isophotes for CN λ3884Å, April 17.394 UT, 1970, $r = 0.830$ AU, $\Delta = 1.039$ AU.

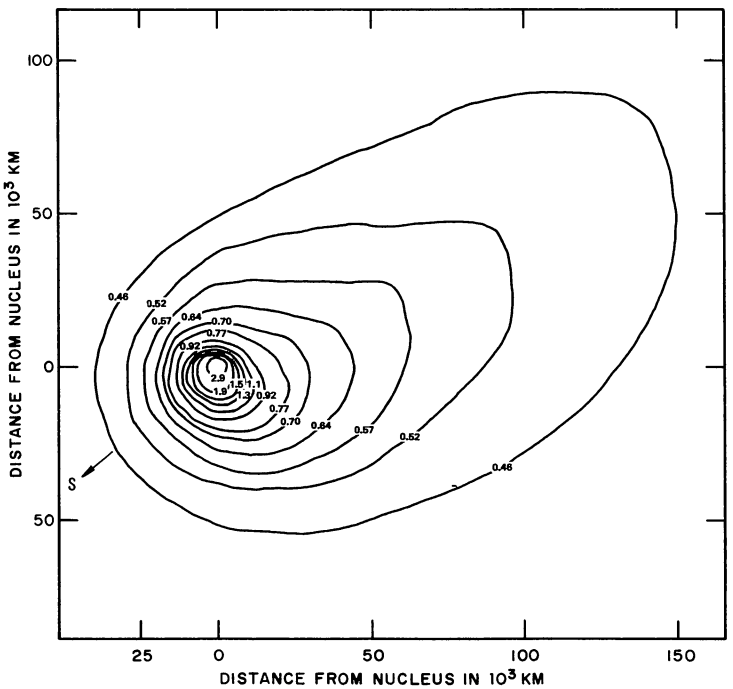

Figure 16 Isophotes for CO^+ λ4267Å, April 17.400 UT, 1970, $r = 0.830$ AU, $\Delta = 1.039$ AU.

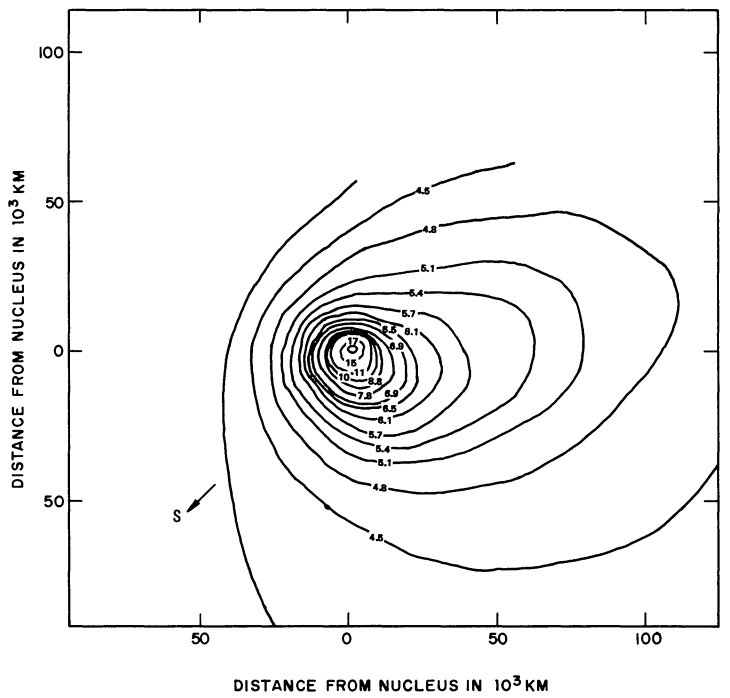

Figure 17 Isophotes for Na λ5893Å, April 17.408 UT, 1970, $r=0.831$ AU, $\Delta=1.039$ AU.

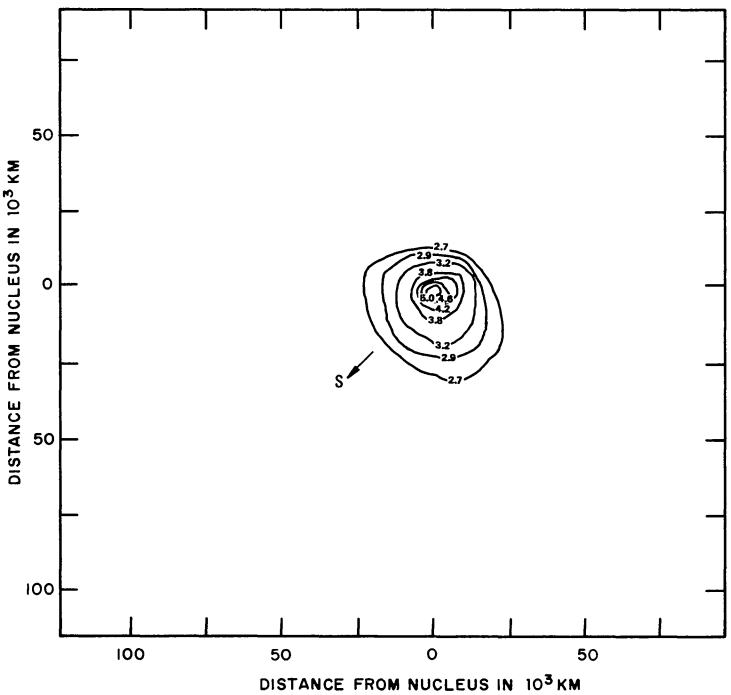

Figure 18 Isophotes for Continuum λ5300Å, April 17.412 UT, 1970, $r=0.831$ AU, $\Delta=1.039$ AU.

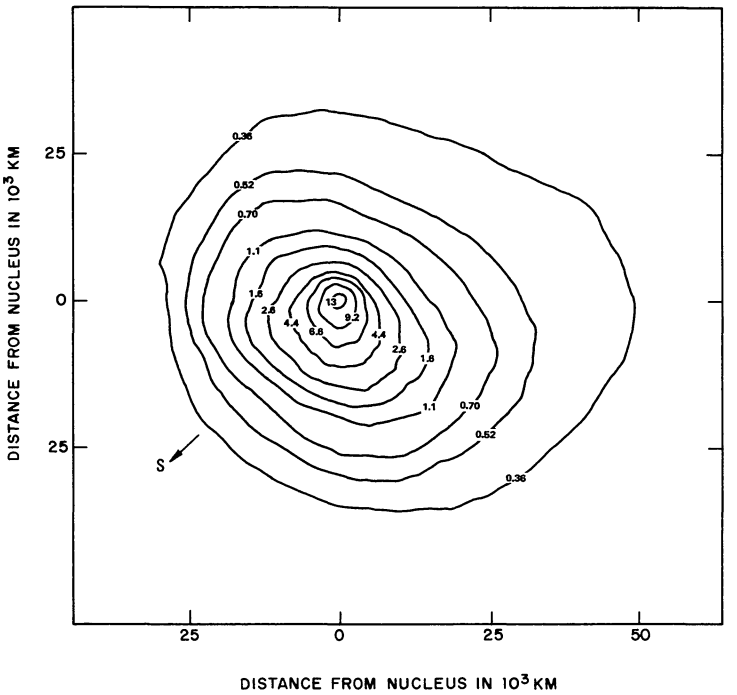

Figure 19. Isophotes for Continuum λ5300Å, April 18.356 UT, 1970, $r = 0.846$ AU, $\Delta = 1.062$ AU.

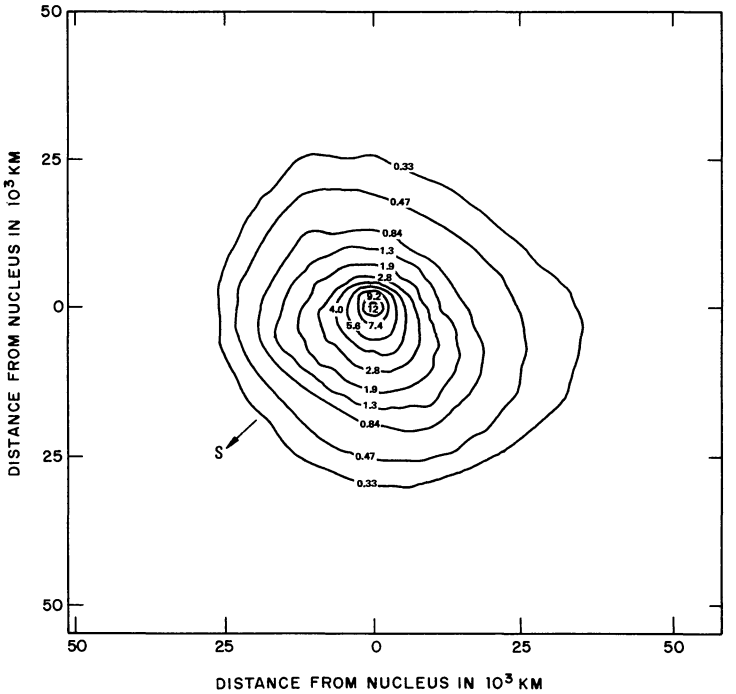

Figure 20 Isophotes for Na λ5893Å, April 18.365 UT, 1970, $r = 0.846$ AU, $\Delta = 1.062$ AU.

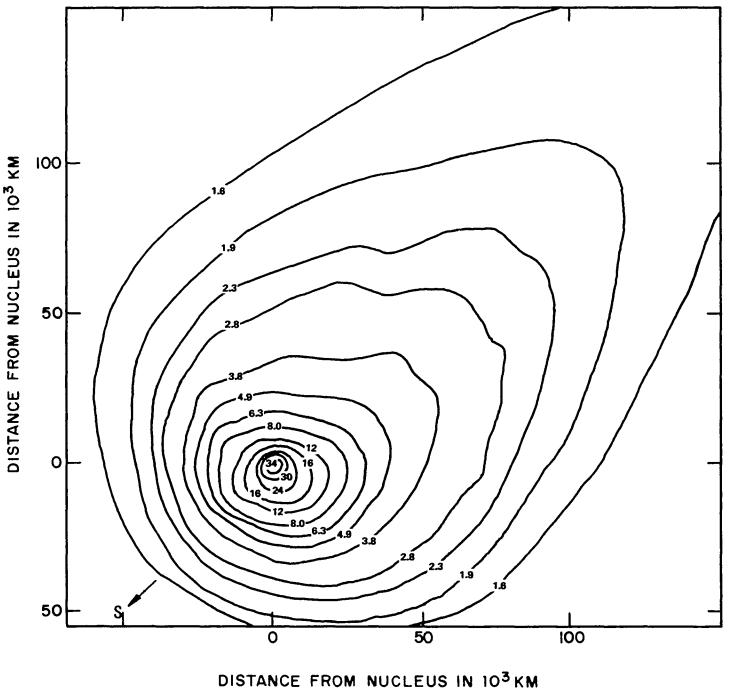

Figure 21 Isophotes for Na λ5893Å, April 18.368 UT, 1970, $r = 0.846$ AU, $\Delta = 1.062$ AU.

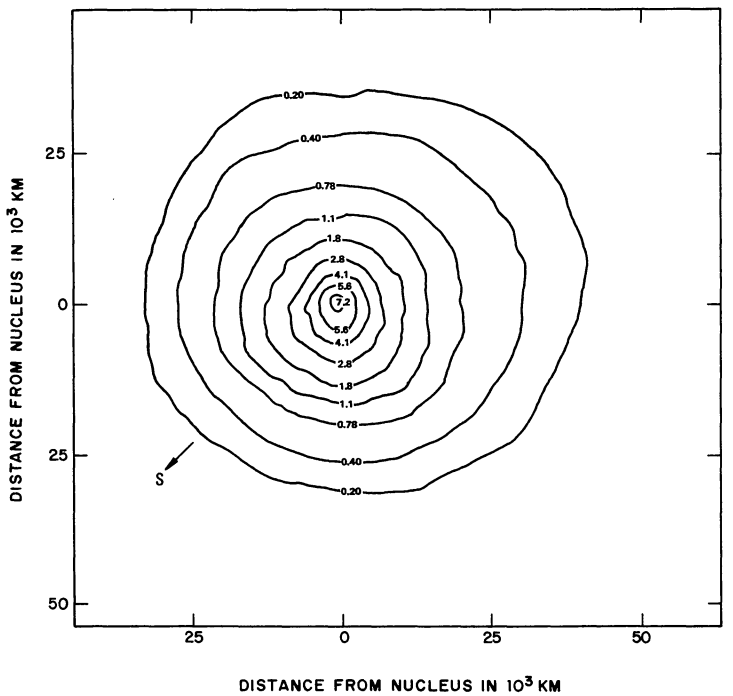

Figure 22 Isophotes for C_2 λ5172Å, April 18.374 UT, 1970, $r = 0.846$ AU, $\Delta = 1.062$ AU.

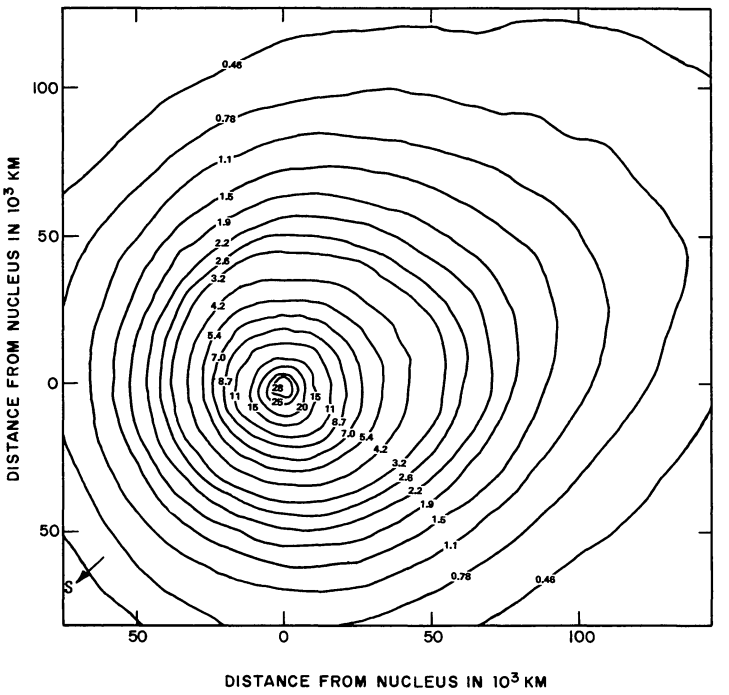

Figure 23 Isophotes for C_2 λ5172Å, April 18.377 UT, 1970, $r = 0.846$ AU, $\Delta = 1.062$ AU.

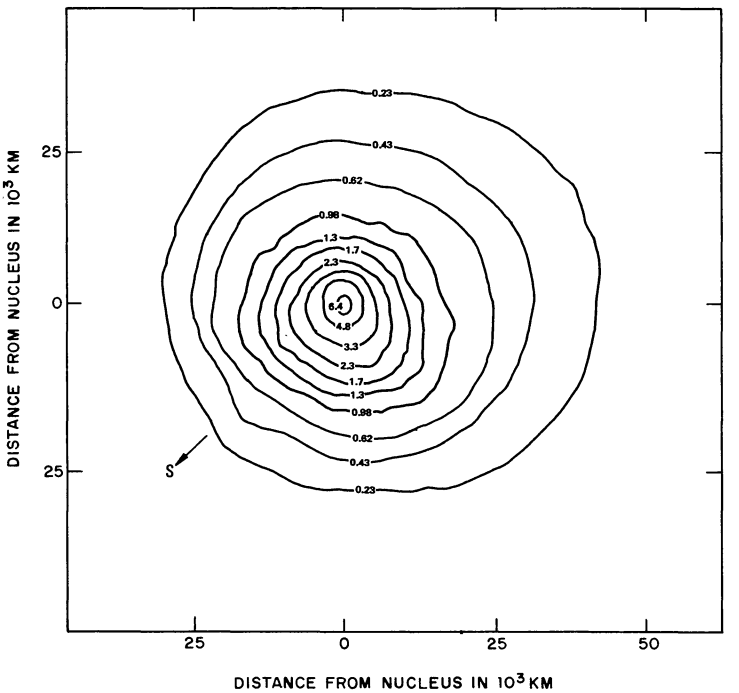

Figure 24 Isophotes for C_2 λ4738Å, April 18.383 UT, 1970, $r = 0.846$ AU, $\Delta = 1.062$ AU.

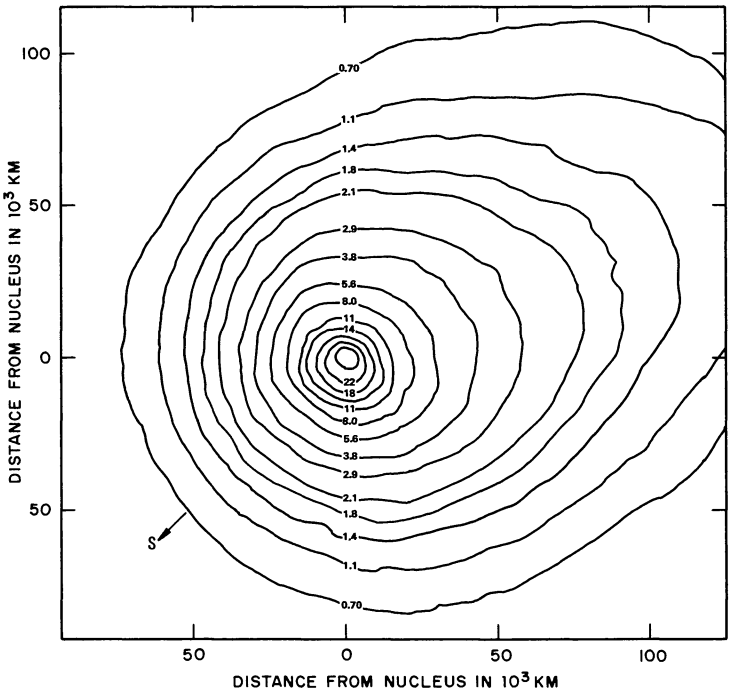

Figure 25 Isophotes for C_2 λ4738Å, April 18.385 UT, 1970, $r=0.846$ AU, $\Delta=1.062$ AU.

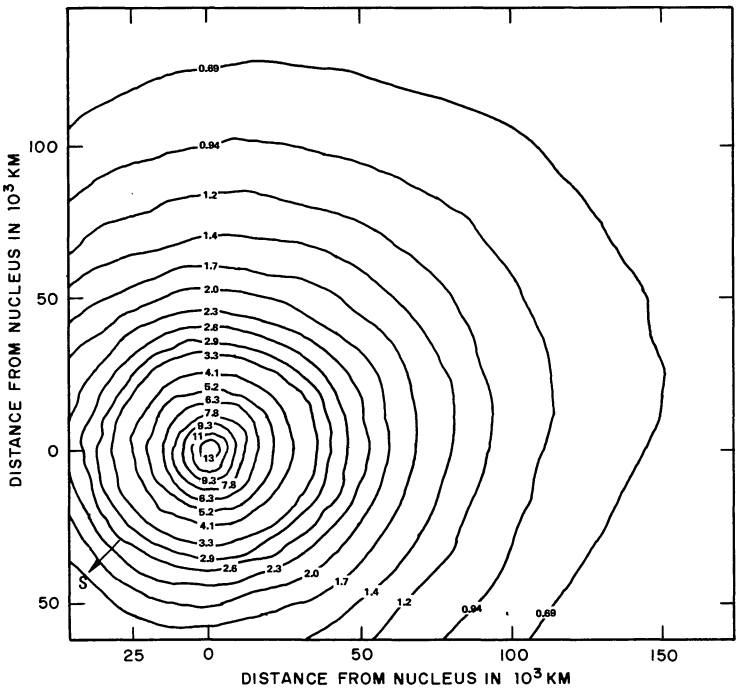

Figure 26 Isophotes for CN λ3884Å, April 18.394 UT, 1970, $r=0.846$ AU, $\Delta=1.062$ AU.

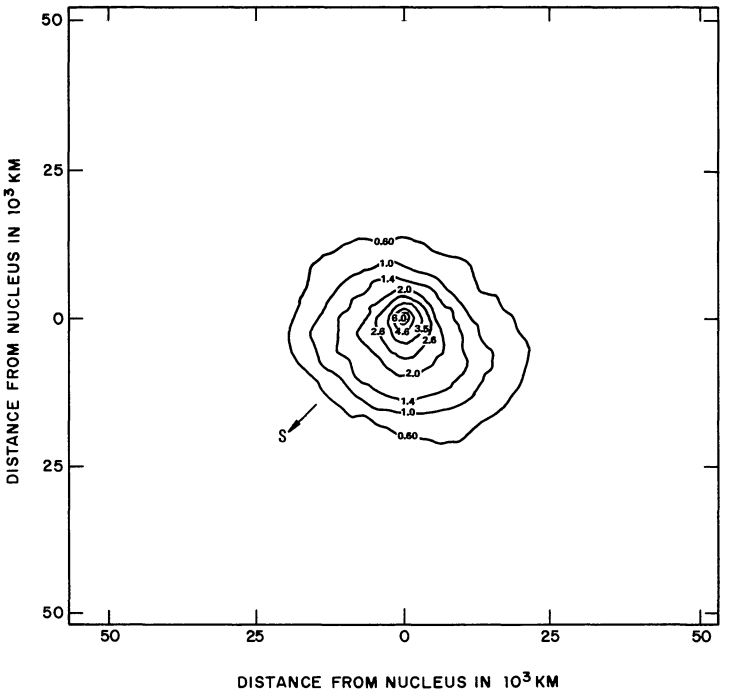

Figure 27 Isophotes for CO^+ λ4267Å, April 18.400 UT, 1970, $r=0.846$ AU, $\Delta=1.063$ AU.

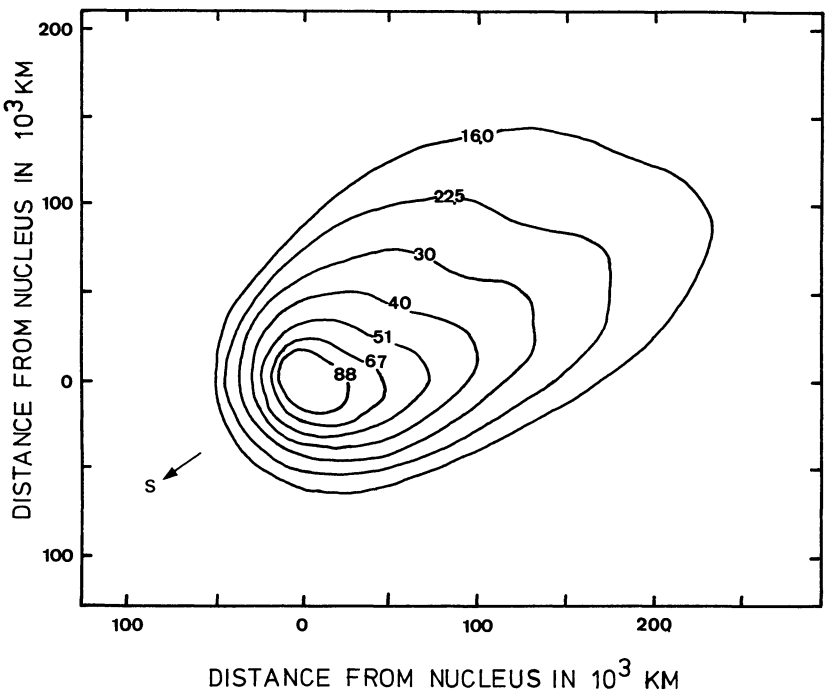

Figure 28 Intensity contours for photograph taken in white light without filter, April 8.12 UT, 1970, $r=0.69$ AU, $\Delta=0.83$ AU.

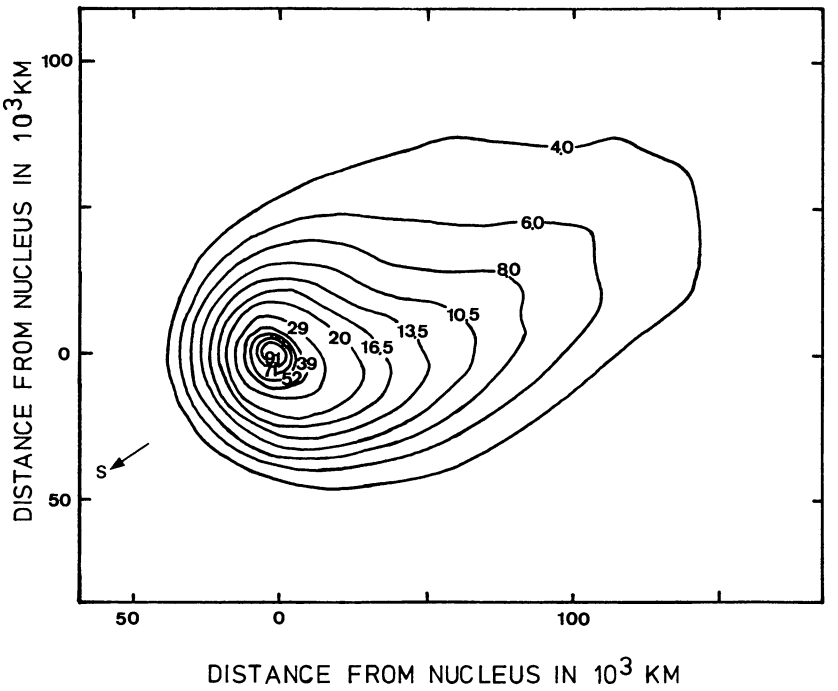

Figure 29 Intensity contours for photograph taken in white light without filter, April 8.142 UT, 1970, $r=0.69$ AU, $\Delta=0.83$ AU.

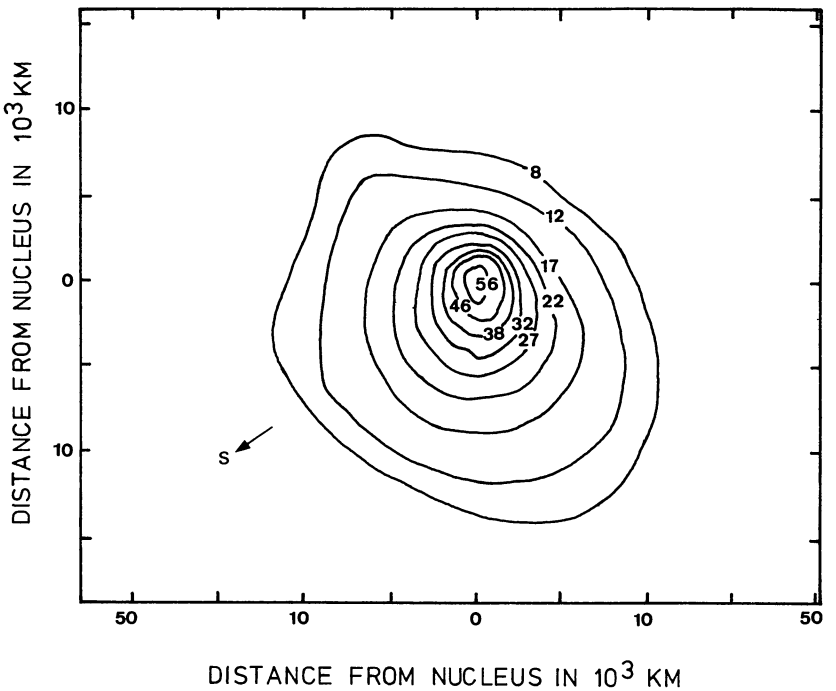

Figure 30 Intensity contours for photograph taken in white light without filter, April 9.086 UT, 1970, $r=0.71$ AU, $\Delta=0.85$ AU.

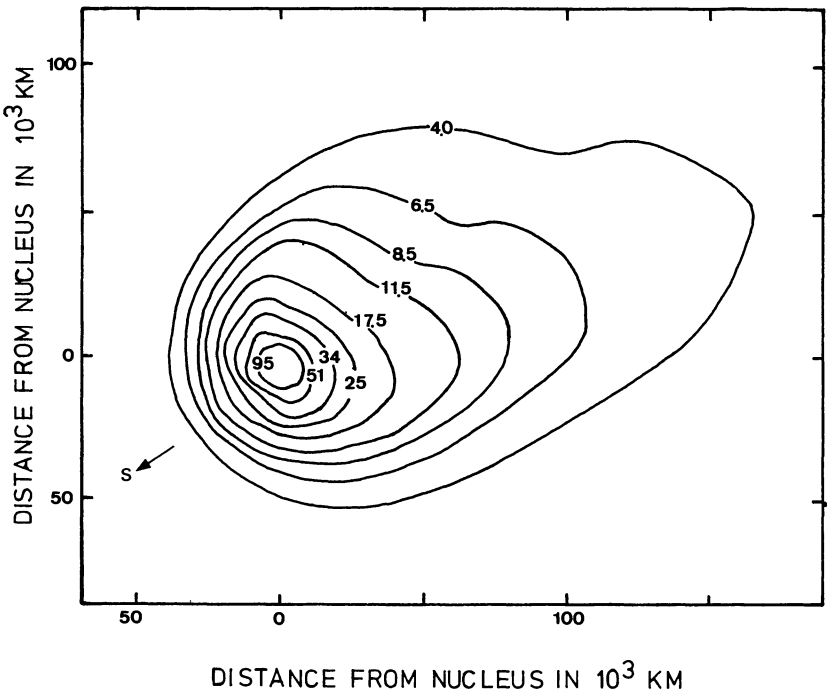

Figure 31 Intensity contours for photograph taken in white light without filter, April 9.099 UT, 1970, $r=0.71$ AU, $\Delta=0.85$ AU.

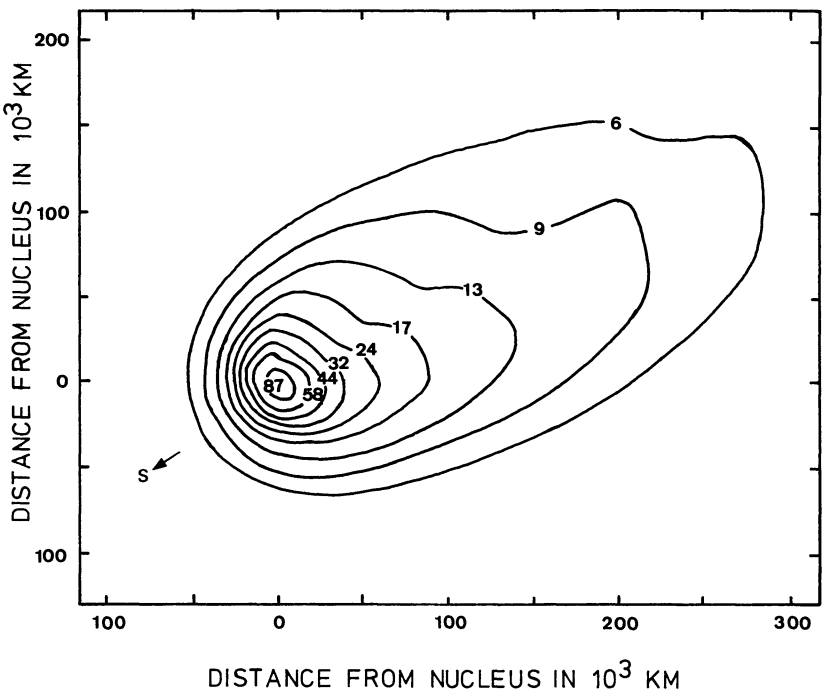

Figure 32 Intensity contours for photograph taken in white light without filter, April 9.110 UT, 1970, $r=0.71$ AU, $\Delta=0.85$ AU.

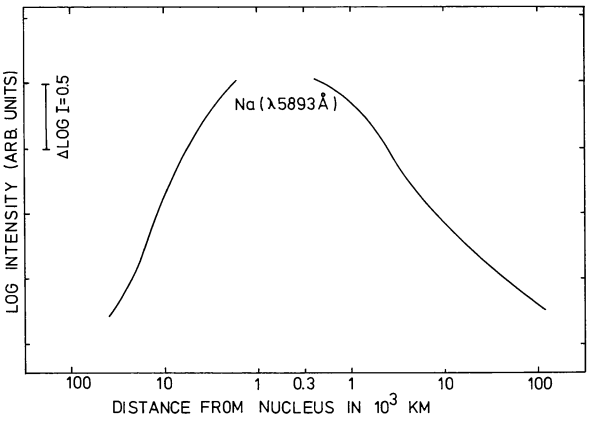

Figure 33 Intensity gradients along the sun-comet line (sun toward the left) for Na λ5893Å, March 28 UT, 1970.

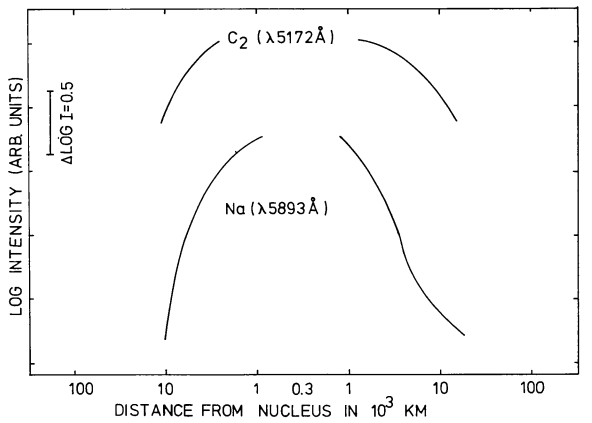

Figure 34 Intensity gradients along the sun-comet line (sun toward the left) for C_2 λ5172Å and Na λ5893Å, March 30 UT, 1970.

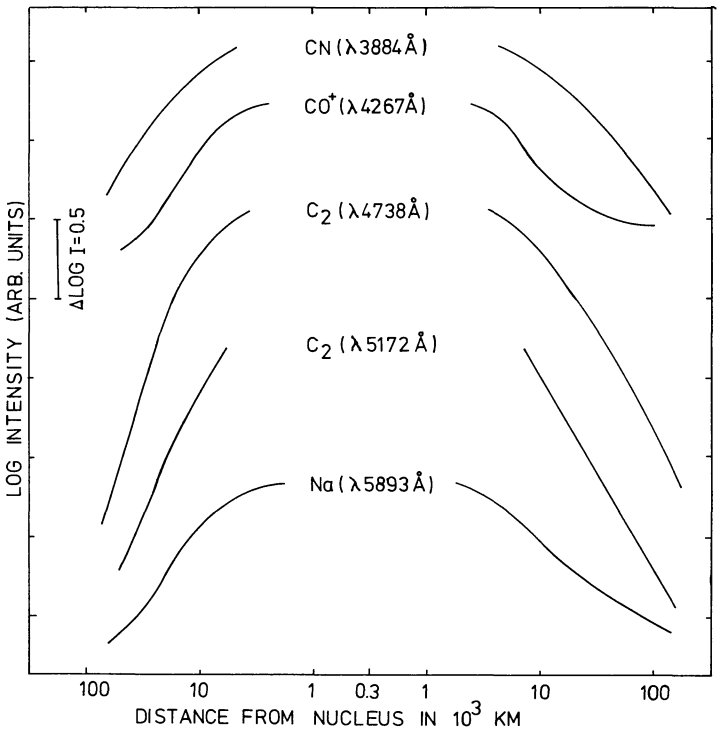

Figure 35 Intensity gradients along the sun-comet line (sun toward the left) for CN λ3884Å, CO^+ λ4267Å, C_2 λ4738Å, C_2 λ5172Å, and Na λ5893Å, April 16 UT, 1970.

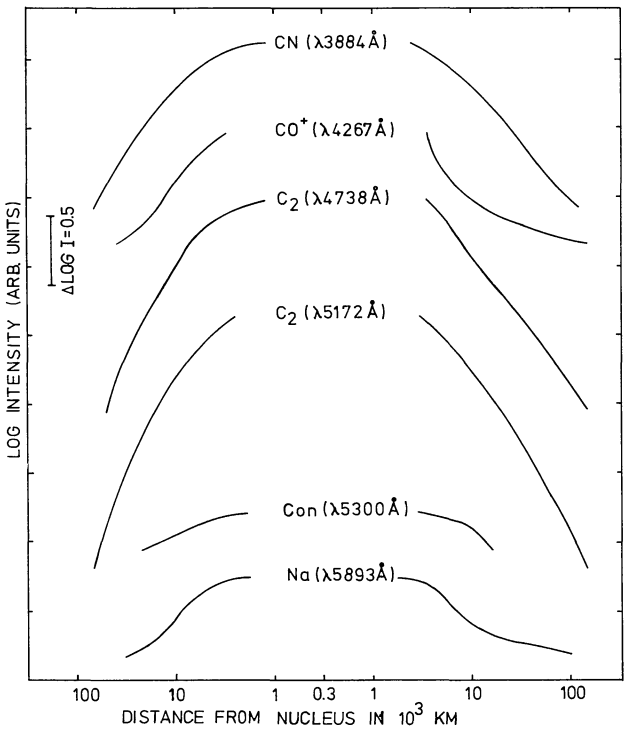

Figure 36 Intensity gradients along the sun-comet line (sun toward the left) for CN λ3884Å, CO^+ λ4267Å, C_2 λ4738Å, C_2 λ5172Å, Continuum λ5300Å, and Na λ5893Å, April 17 UT, 1970.

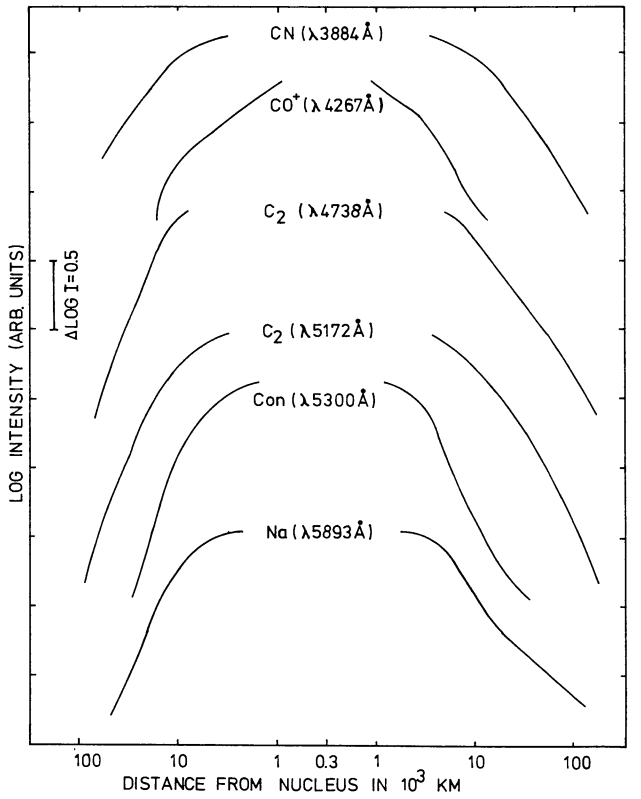

Figure 37 Intensity gradients along the sun-comet line (sun toward the left) for CN λ3884Å, CO^+ λ4267Å, C_2 λ4738Å, C_2 λ5172Å, Continuum λ5300Å, and Na λ5893Å, April 18 UT, 1970.